Türk Mühendislik Araştırma ve Eğitimi Dergisi
**Turkish Journal of Engineering Research and Education**

1(1), 29-37, (2022)

**RESEARCH ARTICLE**

# The Effects of Different Origins NaOH on the Mechanical and Microstructural Properties of Tuff-Based Alkali-Activated Pastes

# *Tüf Esaslı Alkali-Aktive Edilmiş Hamurların Mekanik ve Mikro Yapısal Özelliklerine Farklı Orijinli NaOH'ın Etkileri*

**Mahfuz Pekgöz, İlker Tekin***
Karabük University, Department of Civil Engineering, Karabük, Turkey

**Geliş / Received: 29.04.2022**
**Kabul / Accepted: 30.05.2022**

***Sorumlu Yazar (Corresponding Author) İlker Tekin, ilkertekin@karabuk.edu.tr**

**ABSTRACT:** Turkey has rich deposits in natural stones such as marble and volcanic tuff. These are commonly used as cladding tiles in the construction sector. So, almost 70% wastes are aroused during the production processes of both quarries and factories. These wastes give rise to solid state environmental pollutions in large and micro scales. Alkali-activation method (AAM) is the most effective way to use these wastes in productions like brick manufacturing, and also NaOH is the most common alkali-activator in the production of AAMs. However, the NaOH manufacturing sector is very huge in the world; and there are lots of brands which use different technics. In here, alkali-activated pastes (AAP) contained tuff and travertine were produced with using NaOH as an alkali activator from two different countries in the solutions with 5 Molar and 10 Molar concentrations. All AAPs were cured in laboratory condition at 22±2 °C and 35% R.H. The compressive strength tests were carried out on the 7th, 28th and 90th days of curing period. Moreover, microstructural investigations were performed on AAPs at the age of 90 day. As a result of this study, NaOH from different countries effects the mechanical and microstructural properties. The highest compressive strength is obtained as 46 MPa. It is observed that the AAPs prepared with 5 molar concentration aren't stable sufficiently after 28th days mostly.

**Keywords:** Travertine, volcanic tuff, alkali-activated paste, compressive strength, microstructure

**ÖZ:** Türkiye, mermer ve volkanik tüf gibi doğal taşlar açısından zengin yataklara sahiptir. İnşaat sektöründe genellikle kaplama karosu olarak kullanılırlar. Böylece hem taş ocaklarında hem de fabrikalarda üretim süreçlerinde yaklaşık %70'e yakın atık ortaya çıkmaktadır. Bu atıklar, büyük ve mikro ölçekte katı hal çevre kirliliğine yol açmaktadır. Alkali ile aktive olan malzemeler (AAM'ler), bu atıkları tuğla üretimi gibi bazı üretimlerde kullanmanın en etkili yoludur ve ayrıca AAM'lerin üretiminde NaOH en yaygın alkali aktivatördür. Ancak, NaOH imalat sektörü dünyada çok büyüktür ve farklı teknikler kullanan birçok marka bulunmaktadır. Burada iki farklı ülkeden temin edilmiş granül halde NaOH alkali aktivatör olarak 5 Molar ve 10 Molar konsantrasyonlarda çözelti ile tüf ve traverten içeren alkali ile aktive edilmiş hamurlar (AAP) üretilmiştir. Tüm AAP'ler laboratuvar koşullarında 22±2 °C ve %35 R.H'de kürlenmiştir. Kür periyodunun 7., 28. ve 90. günlerinde basınç dayanımı testleri yapılmıştır. Aynı zamanda 90 gün yaşındaki AAP'lerde mikro yapı incelemeleri de gerçekleştirilmiştir. Bu çalışma sonucunda farklı ülkelerden NaOH hem mekanik hem de mikroyapısal özelliklere etki etmektedir. En yüksek basınç dayanımı 46 MPa olarak elde edilmiştir. 5 molar konsantrasyonla hazırlanan AAP'lerin çoğunlukla 28. günden sonra yeterince stabil olmadığı gözlendi.

**Anahtar Kelimeler:** Traverten, volkanik tüf, alkali aktifleştirilmiş hamur, basınç dayanımı, mikro yapı.

# 1. INTRODUCTION

Cement, brick, clay tile, ceramic tile like materials used in the construction industry require much energy in the production. The process of these production is essentially led to a considerable amount of $CO_2$ releasing into atmosphere. For example, the latest data revealed that $CO_2$ emissions attained 180.000 tons a year for ceramic cladding tile production [1]. Since 2000, cement production has increased almost 78%, so this has triggered of the anthropogenic $CO_2$ emissions to 5-8% [2]. However, energy requirement of brick, clay tile, and ceramic tile productions are nearly 2.25, 4.88 and 9.02 times higher than that of cement production, respectively [3]. Recently, alkali-activation method can be one of the most efficient alternatives to the energy required materials soon, since its production emit lower $CO_2$ and more green materials will be able to product by this method.

Alkali-activated materials (AAM) or geopolymers are produced by the polymerization reactions between various sources of solid aluminosilicate and alkaline media. Aluminosilicate sources such as fly ash, slag, metakaolin, volcanic tuff, trass, red mud can be found from industrial wastes frequently. Ground Granulated Blast Furnace Slag (GGBFS) [4], Metakaolin (MK) [5], Volcanic tuff [6,7] and Fly Ash (FA) [8] are the major precursors utilized in studies about AAMs [9]. In order to produce AAMs alkaline activators, which contain $Na_2O$, $K_2O$, MgO, CaO, earth metals water glasses, have to be used to trigger the polymeric reaction mechanisms. Because pozzolanic materials have low reaction capacity, and they need alkaline substance with moisture in condition. Sodium hydroxide (NaOH), potassium hydroxide (KOH), sodium silicate ($Na_2SiO_3$), sodium carbonate ($Na_2CO_3$), sodium sulfate ($Na_2SO_4$), and calcium hydroxide ($Ca(OH)_2$) are the most common alkaline-activators [10]. All of these, except NaOH, emit $CO_2$ to the atmosphere during manufacturing. NaOH can be manufactured by using two methods: 1) By using the method of electrolysis of brine (NaCl), 2) By burning method of $NaCO_3$. First method, electrolysis of brine, is preferred mostly in NaOH production, and this process releases only $Cl_2$ and $H_2$. The second one causes more $CO_2$ emissions during production, but some companies still use this method [11]. Therefore, activation process can be varied by changing production method because of varies total inner energy of NaOH. Even if $Na_2CO_3$ can be used as an alkaline activator, the activation capacity of $Na_2CO_3$ is lower than NaOH. Moreover, each process has some effects to the activator quality; however, there isn't any information about it in the existing literature. The main reaction products in AAMs are sodium-aluminosilicate-hydrate (N-A-S-H) and calcium-aluminosilicate-hydrates (C-A-S-H) besides hydrotalcite and other crystalline phases [12].

Turkey has rich natural stone deposits with various volcanic tuffs and travertine resources. Existing reserves are 3,872,000,000 $m^3$ in marble [13] and 155,000 $km^2$ in natural pozzolana, although there is some missing in this information because of the limitation of determining the sub structure of volcanic rocks [14]. Due to the technical constraints and the geological environment, yield efficiency rarely exceeded 10% in quarry mining and travertine facing production. In countries which famous in travertine production such as China, Turkey, Italy, Greece and Spain, large amounts of macro and micro wastes are observed as debris during the quarrying and stone cutting processes [15]. It is reported that 90% of the micro-sized travertine wastes formed by sawing during the production of marble coating tile pass through the 200 μm sieve [16]. Moreover, landfill areas are not enough to collect these wastes since this destruct the agricultural areas.

In this study, the main aim is to determine the effect of sodium hydroxides (NaOH) with different origins on mechanical and microstructural properties of AAPs contained volcanic tuff and travertine wastes. With this objective, AAPs were manufactured using wastes of travertine and tuff production collected from Bayburt region of Turkey. To support the objective of this study, saw cut wastes with sized below 200 microns is used. In preparing of AAPs, NaOH was used as an alkali-activator because it is the best alkaline-activator due to the atomic instability of $Na^+$ ions. In the literature, NaOH is mostly used on production of geopolymer, but there is no information about using different origin of NaOH. With this scope, the following tests are conducted on alkaline-activated pastes (AAP) such as compressive strength, microscopic and mineralogical analyses.

# 1. MATERIAL AND METHODS

## *1.1 Materials*

In the experimental study, volcanic tuff (VT) and travertine waste (TW) in powder forms were used in the preparing AAPs. Zeolitic volcanic tuff and travertine wastes were collected from Bayburt province in the northeast of Turkey. Initially, these substances were crushed and grinded by using laboratory type crusher and horizontally ball mill to reduce the particle size below 100 µm. Chemical compositions of VT and TW are given in Table 1. According to Table 1, alumina, silicate, and ferritin amount of VT is totally higher than 80% and its CaO content is lower than 10%. Thus, VT shows pozzolanic behavior [17]. Moreover, alkaline substance amount is almost 8%. However, LOI value is approximately 10%, and this value is slightly high for volcanic tuff. $CO_3$ or $SO_2$ like substances can be caused this LOI value. France (Type I) and China (Type II) based sodium hydroxides (NaOH), which have two different densities, with 99.9% purity was used in AAP as alkaline activator. The information about the production styles of NaOH did not get from the companies because of its hide process systems.

**Tablo 1:** Chemical and physical properties of VT and TW.

| **Oxides (%)** | **VT** | **TW** |
|---|---|---|
| $SiO_2$ | 68.92 | 0.70 |
| $Al_2O_3$ | 11.96 | - |
| $Fe_2O_3$ | 0.34 | 0.20 |
| CaO | 3.85 | 55.10 |
| MgO | 1.29 | 0.20 |
| $SO_3$ | 0.21 | - |
| $Na_2O$ | 0.23 | - |
| $K_2O$ | 2.38 | - |
| LOI* | 10.13 | 43.50 |
| Total | 99.31 | 99.70 |

Particle size distribution and mineralogic structure analysis of VT are shown Figure 1 and Figure 2, respectively. According to the Figure 1, 90% of VT pass from 100-micron size, and 50% of VT pass from 30-micron size. Approximately 25% of VT is lower than 10-micron. Specific gravities of ZT and TW are 2.42 g/cm$^3$ and 2.70 g/cm$^3$, and specific surface area of ZT and TW are 10845 g/cm$^3$ and 2720 g/cm$^3$. Even if the particle size distributions of both substances are similar, specific surfaces of both are considerably different because of the microstructures of substances. For example, VT has zeolitic structure, so it has meso-porous structure.

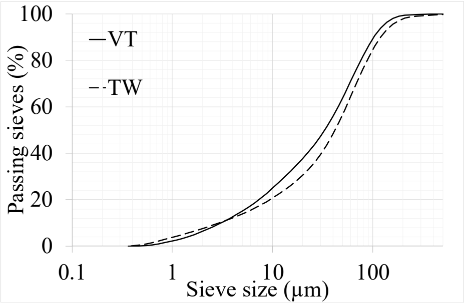

**Figure 1:** Particle size distributions of wastes

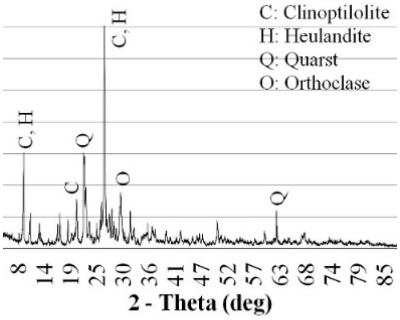

**Figure 2:** XRD analysis of BSW from METU Merlab

## *1.2 Experimental Methods*

In this study, VT and TW were used as binder and filler materials to product AAPs. Within this scope, mix design parameters of all AAP are given in Table 2. According to this table, the initial letter of the codes indicates the powder state volume proportions by solid materials shown as 0.4:0.6, 0.6:0.4, and 0.8:0.2 (VT/TW) for A, B, and C respectively. The reason of determining these ratios is to provide stoichiometry to supply chemical reactions sufficiently to obtain both geopolymeric structure and high compressive strength. Since VT doesn't contain calcium ions satisfactorily, authors were used TW as high as possible to react the VT in alkaline media. In addition, the previous study by Tekin (2016) [6] was a pioneer in determining the material ratios. The second designation of the codes indicates the concentration of NaOH in the molarity of the solutions given as follows: ***5***: 5 M, and ***10***: 10 M. The three designation of the codes indicates the type of NaOH given as follows: ***I***: Type I NaOH, and ***II***: Type II NaOH. During experimental studies, standard consistency is fixed in 20±2 cm for all series according to flow table diameter to make the evaluations easier. So, solution/powder (S/P) ratios are changed significantly because of the different surfactant effect of NaOH origins.

**Tablo 2:** Mix proportions of AAPs prepared with VT and TW.

| AAPs | NaOH Types | Solution molarity | S/P | VT | TW |
|---|---|---|---|---|---|
| A5I | I | 5 | 0.28 | 0.27 | 0.46 |
| B5I | I | 5 | 0.30 | 0.40 | 0.30 |
| C5I | I | 5 | 0.32 | 0.53 | 0.15 |
| A10I | I | 10 | 0.34 | 0.24 | 0.41 |
| B10I | I | 10 | 0.36 | 0.37 | 0.28 |
| C10I | I | 10 | 0.37 | 0.49 | 0.14 |
| A5II | II | 5 | 0.25 | 0.28 | 0.47 |
| B5II | II | 5 | 0.26 | 0.42 | 0.32 |
| CII | II | 5 | 0.29 | 0.55 | 0.16 |
| A10II | II | 10 | 0.28 | 0.27 | 0.46 |
| B10II | II | 10 | 0.29 | 0.40 | 0.30 |
| C10II | II | 10 | 0.32 | 0.53 | 0.15 |

Solutions with different concentrations were prepared before preparation of AAPs. Meanwhile, pH value of the solution increased up to 14 and its temperature boosted to approximately 85 °C till all particles of NaOH dissolved. In the preparation of AAPs, the solution and VT were mixed together for 60 s, afterward TW was added into the mix, and all substances were mixed in two steps sequentially (1st step: 30 s at slow speed (1400 rpm) 2nd step: 90 s at speed (2800 rpm)). NaOH solutions were used in 22±2 °C in ambient temperature with 5M and 10M concentration. 12 groups of AAPs were produced using this mix procedure. AAP was cast in 50x50x50 mm sized steel molds to determine the compressive strength according to ASTM C109 [18]. Compressive strength and water absorption tests were carried out on the hardened paste at the age of 2nd, 28th and 90th days, in addition scanning electron microscopy (SEM) analyzes were performed out on the hardened pastes on 90th day.

## 2. Results and Discussion

### 2.1 *Fresh state properties of AAPs*

One of the flow table examination of 10M AAP with Type II NaOH is shown in **Figure 3**. In here, AAP with Type II NaOH causes the similar flowability to the AAP with Type I NaOH although S/P ratio was chosen in lesser ratio. Therefore, compressive strength increased dramatically. Fresh state AAP with 10M concentration is shown in Figure 3 as dense cohesive and plastic consistency. It is determined that this is the limit consistency value of AAPs to settled with lesser energy. Figure 4 shows the correlation between S/P and VT ratios. According to the S/P ratios of AAPs, as VT ratio increases, S/P ratio increases due to the higher specific surface of VT. It is clearly seen that the Type II NaOH is more effective for workability with lesser S/P ratios.

**Figure 3:** Flow table test result of AAP with Type II NaOH at lesser S/P ratio

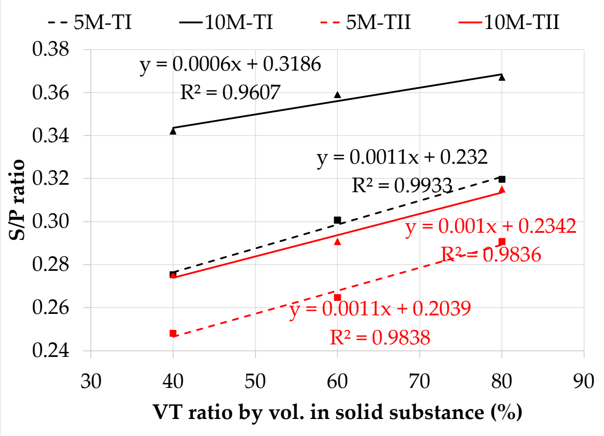

**Figure 4:** Correlation between S/P and VT ratios

### 2.2 *Compressive strength test results of AAPs*

Compressive strength test results of hardened AAPs are given in Figure 5. According to the experimental results, the highest late compressive strength is observed as 46 MPa on the C10II with 10M 80% VT contents and prepared by using Type II NaOH. Minimum compressive strengths are observed on the 5M AAPs for all durations. Compressive strength developments of 10M AAPs based on duration are different by changing substance ratios. For example, on the 10M AAPs with Type II NaOH, CaO from travertine causes increase in compressive strength more than others after 7th day. However, as CaO ratio decreases, early and late compressive strengths increases by time. In these AAPs, the reason of higher compressive strengths can be attributed to the S/P ratio firstly, but this is also resulted from the origin of NaOH. NaOH origin effects to compressive strengths by increasing concentrations. In here, 10M concentration is more effective for compressive strengths than 5M NaOH.

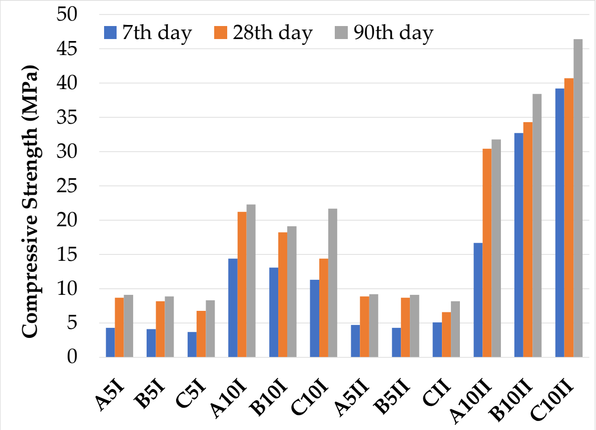

**Figure 5:** Compressive strength test results of AAPs

Compressive strengths of 10M Type I NaOH used AAPs are roughly 3 times higher than 5M Type I NaOH used AAPs, and similarly Type II NaOH used AAPs with 10M concentration are also 3-7 times higher than 5M Type I NaOH used AAPs. Hence, these results show that the Type II NaOH is more active than Type I NaOH. Pastes with 5M concentrated AAPs are carbonated higher than 10M concentrated AAPs as shown in Figure 6. In here, all surfaces of 5M AAPs are carbonated by leaching of NaOH [6]. Therefore, compressive strength values are obtained as lower levels.

On the other hand, early relative compressive strength developments based on 28th day of AAPs with 5M concentration are calculated between 49%-77%, while early relative compressive strength developments of AAPs with 10M concentration are calculated between 54%-96%. Similarly, late relative compressive strength developments based on 28th day of AAPs with 5M concentration are calculated between 104%-124%, while late relative compressive strength developments of AAPs with 10M concentration are calculated between 104%-150%. Relative compressive strength development of Type II NaOH based AAPs is the highest among all AAPs.

**Figure 6:** AAP specimens with different concentrations

### 2.3 *Microstructural analyses of AAPs*

Microstructural analyses are conducted by imaging scanning electron microscopy (SEM) in the mineralogy and Petrography Laboratory of "General Directorate of Mineral Research and Exploration (MTA in Turkish)". Initially, SEM images are observed, and some regions and points were analyzed by using Energy Dispersive Spectrum (EDS). EDS gives the elemental analyses of any point, and so some of definitive important structures can be determined or foreseen easily. Microscopically investigations are performed from Figure 7 – 10. Figure 7 and 8 shows the 10M Type II NaOH based AAPs, Figure 9 and 10 shows the 10M Type I based AAPs. In these AAPs VT ratio is used 60%. All figures are depicted by 2 SEM images with at least 1 EDS analysis. SEM images are given as macro and micro scale in some regions.

Figure 7 shows a void and its detail of B10II AAP specimen. The void is full of hexagonal structures. These are defined as N-(C)-A-S-H with some percentage like Si/Al: 2.05. But $Na^+$ ions are too much in this structure, so it can be led to the shape. Because on the surface between lattices has different apparent like amorphous phase. On the surface Si/Al ratio is more different according to lattice form, it is almost 4 (two times bigger than lattice form). And this observation is usual for the B10II AAP. The general structure of this specimen especially in porous system is full of lattice forms like this.

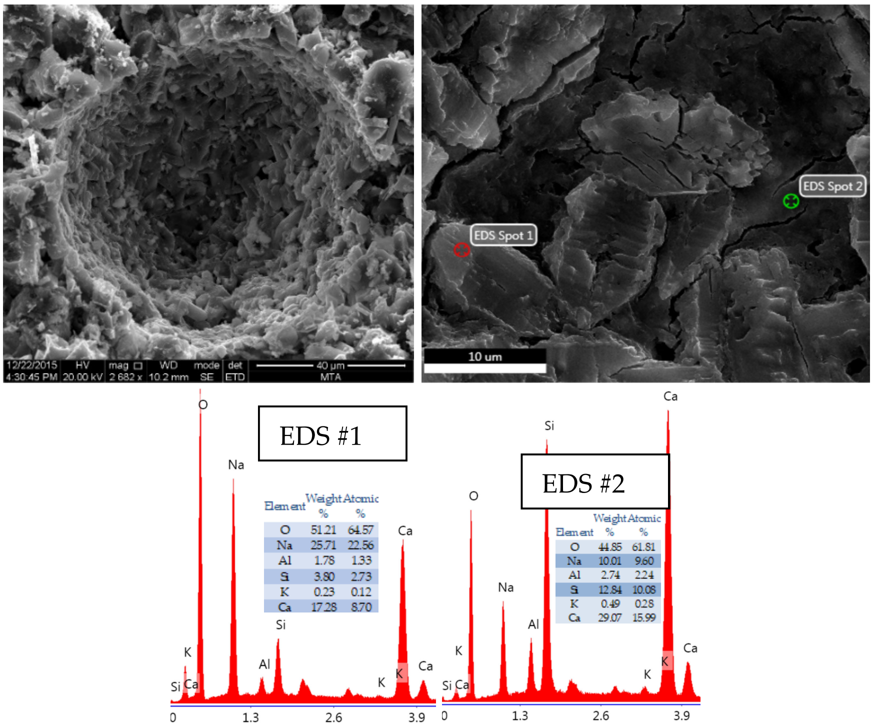

EDS #1

| Element | Weight % | Atomic % |
|---|---|---|
| O | 51.21 | 64.57 |
| Na | 25.71 | 22.56 |
| Al | 1.78 | 1.33 |
| Si | 3.80 | 2.73 |
| K | 0.23 | 0.12 |
| Ca | 17.28 | 8.70 |

EDS #2

| Element | Weight % | Atomic % |
|---|---|---|
| O | 44.85 | 61.81 |
| Na | 10.01 | 9.60 |
| Al | 2.74 | 2.24 |
| Si | 12.84 | 10.08 |
| K | 0.49 | 0.28 |
| Ca | 29.07 | 15.99 |

**Figure 7:** SEM images and EDS analyses of B10II from a voids

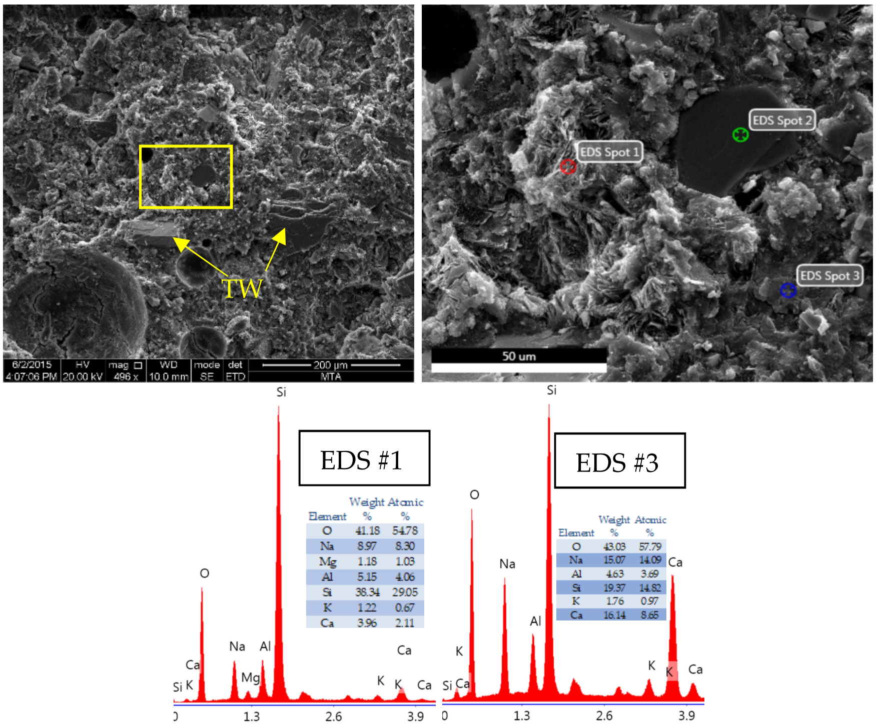

EDS #1

| Element | Weight % | Atomic % |
|---|---|---|
| O | 41.18 | 54.78 |
| Na | 8.97 | 8.30 |
| Mg | 1.18 | 1.03 |
| Al | 5.15 | 4.06 |
| Si | 38.34 | 29.05 |
| K | 1.22 | 0.67 |
| Ca | 3.96 | 2.11 |

EDS #3

| Element | Weight % | Atomic % |
|---|---|---|
| O | 43.03 | 57.79 |
| Na | 15.07 | 14.09 |
| Al | 4.63 | 3.69 |
| Si | 19.37 | 14.82 |
| K | 1.76 | 0.97 |
| Ca | 16.14 | 8.65 |

**Figure 8:** SEM images and EDS analyses of B10II from surface.

Moreover, there are lots of cracks on the lattice and surface structures because of drying shrinkage. This causes discontinuity of forms and so it causes decreasing compressive strengths.

On the surface of B10II AAP shown in Figure 8, there are lots of different forms like leaf (EDS#1) and lattice (EDS#3) structured. On the right SEM image of Figure 8 is a magnified one from the rectangular area. EDS#2 is a TW below 50 micron, EDS#1 is a leaf like form and EDS#3 depicts an amorphous structure. In here, there are some lattice forms like in porous areas. On the point of EDS#1, Si/Al ratio is above 7 and in here $Ca^{2+}$ and $Na^{+}$ ions are quietly low. So, this can be non-reacted clay structures in VT. However, on the EDS#3 point, Si/Al ratio is approximately 4 and alkaline substance like $Na^{+}$ and $Ca^{2+}$ are higher than EDS#1 point. This can be attributed if there is high ratio alkaline in aluminosilicate structures, it can generate geopolymeric forms like N-A-S-H or N-(C)-A-S-H. in these forms $Ca^{2+}$ ions from TW joined to the activation reactions although travertine is an inert material. This can be attributed that the particle sizes is more important to determine the reactivity or inert behaviors of CaO based materials like travertine.

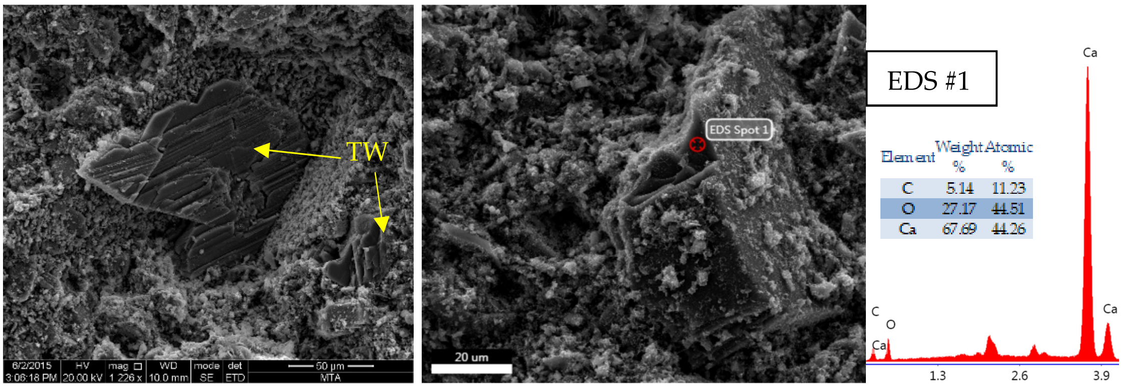

| Element | Weight % | Atomic % |
|---|---|---|
| C | 5.14 | 11.23 |
| O | 27.17 | 44.51 |
| Ca | 67.69 | 44.26 |

**Figure 9:** SEM images and EDS analyses of B10I from surface.

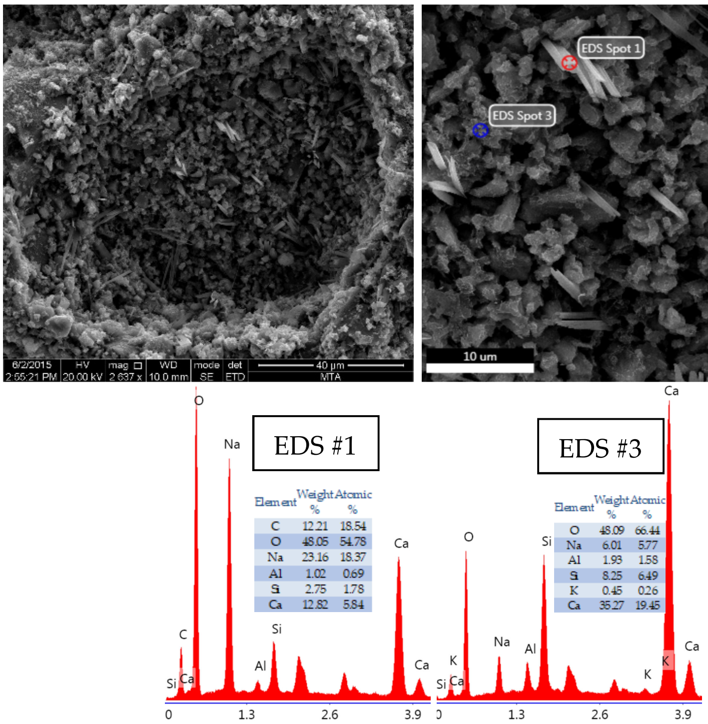

EDS #1

| Element | Weight % | Atomic % |
|---|---|---|
| C | 12.21 | 18.54 |
| O | 48.05 | 54.78 |
| Na | 23.16 | 18.37 |
| Al | 1.02 | 0.69 |
| Si | 2.75 | 1.78 |
| Ca | 12.82 | 5.84 |

EDS #3

| Element | Weight % | Atomic % |
|---|---|---|
| O | 48.09 | 66.44 |
| Na | 6.01 | 5.77 |
| Al | 1.93 | 1.58 |
| Si | 8.25 | 6.49 |
| K | 0.45 | 0.26 |
| Ca | 35.27 | 19.45 |

**Figure 10:** SEM images and EDS analyses of B10I from a void.

On the Figure 9 and Figure 10, surface and a void of Type I NaOH based AAP can be seen, respectively. Particulated forms are clearly observed on both figures. These particles are made of from N-(C)-A-S-H structures, and they appeared tidy forms like zeolitic structures. However, in these forms Si/Al ratios are roughly 3.5 with lesser $Na^+$ (~6%) and higher $Ca^{2+}$ ions (19.45% by atomic weight). In here, potassium is also observed on EDS analysis. Particles are cut off by the rod like lattice forms defined by EDS#1 as can be obviously seen on the right side of Figure 10. These rod like lattice forms have very different elemental structure in terms of both Si/Al and alkaline ratios. Si/Al ratio of these structures are 2.6 and $Ca^{2+}$ ions are approximately 3 times lesser than $Na^+$. these separated particulate structures cause decreasing the compressive strength as well.

## 3. CONCLUSIONS

The conclusions of this study are given below:

1. The highest late compressive strength of the AAPs is obtained 46 MPa on C10II.

2. Compressive strengths of AAPs with 10M NaOH are higher 4 times than the AAPs with 5M NaOH.

3. Origin of NaOH is important for both compressive strength and microstructural forms.

4. While bigger particles of travertine play a role as an aggregate in AAP body, smaller particles of travertine play a role as a reactant material.

5. Although, compressive strength of VT as a rock is approximately 35 MPa [19], after grinded VT is blended with travertine dust by using alkali-activated method, the new material properties such as compressive strength and microstructure have improved.

## 4. ACKNOWLEDGEMENT

This study is funded by TÜBİTAK project no: 213M450.

## 5. REFERENCES

[1] J. Peng, Y. Zhao, L. Jiao, W. Zheng, L. Zeng, "CO2 Emission Calculation and Reduction Options in Ceramic Tile Manufacture-The Foshan Case," Energy Procedia., vol. 16, pp. 467–476, 2012. https://doi.org/10.1016/J.EGYPRO.2012.01.076.

[2] A.R. Sakulich, "Reinforced geopolymer composites for enhanced material greenness and durability," Sustain. Cities Soc., vol. 1, pp. 195–210, 2011. https://doi.org/10.1016/J.SCS.2011.07.009.

[3] G. Hammond, C. Jones (2008). Inventory of carbon & energy (ICE) Version 1.6a. [Online]. Available: www.bath.ac.uk/mech-eng/sert/embodied.

[4] M.J. Nadoushan, P. Dashti, S. Ranjbar, A.A. Ramezanianpour, A.M. Ramezanianpour, R. Banar, "RSM-based Optimized Mix Design of Alkali-activated Slag Pastes Based on the Fresh and Hardened Properties and Unit Cost," J. Adv. Concr. Technol., vol. 20, pp. 300–312, 2022. https://doi.org/10.3151/JACT.20.300.

[5] M.S. Saif, M.O.R. El-Hariri, A.I. Sarie-Eldin, B.A. Tayeh, M.F. Farag, "Impact of Ca+ content and curing condition on durability performance of metakaolin-based geopolymer mortars," Case Stud. Constr. Mater., vol. 16, pp. 922, 2022. https://doi.org/10.1016/J.CSCM.2022.E00922.

[6] I. Tekin, "Properties of NaOH activated geopolymer with marble, travertine and volcanic tuff wastes," Constr. Build. Mater., vol. 127, pp. 607–617, 2016. https://doi.org/10.1016/J.CONBUILDMAT.2016.10.038.

[7] I. Tekin, O. Gencel, A. Gholampour, O.H. Oren, F. Koksal, T. Ozbakkaloglu, "Recycling zeolitic tuff and marble waste in the production of eco-friendly geopolymer concretes," J. Clean. Prod., vol. 268, pp. 122298, 2020. https://doi.org/10.1016/J.JCLEPRO.2020.122298.

[8] L. Li, Y. Wei, Z. Li, M.U. Farooqi, "Rheological and viscoelastic characterizations of fly ash/slag/silica fume-based geopolymer," J. Clean. Prod., vol. 354, pp. 131629, 2022.

https://doi.org/10.1016/J.JCLEPRO.2022.131629.

[9] Z. Sun, A. Vollpracht, "Isothermal calorimetry and in-situ XRD study of the NaOH activated fly ash, metakaolin and slag," Cem. Concr. Res., vol. 103, pp. 110–122, 2018. https://doi.org/10.1016/J.CEMCONRES.2017.10.004.

[10] H. Ye, L. Huang, Z. Chen, "Influence of activator composition on the chloride binding capacity of alkali-activated slag," Cem. Concr. Compos., vol. 104, pp. 103368, 2019. https://doi.org/10.1016/J.CEMCONCOMP.2019.103368.

[11] J. Speight, "Chemical Process and Design Handbook," McGraw-Hill Education, 2002.

[12] H. Ye, "Nanoscale attraction between calcium-aluminosilicate-hydrate and Mg-Al layered double hydroxides in alkali-activated slag," Mater. Charact., vol. 140, pp. 95–102, 2018. https://doi.org/10.1016/J.MATCHAR.2018.03.049.

[13] M. Yavuz Çelik, E. Sabah, "Geological and technical characterisation of Iscehisar (Afyon-Turkey) marble deposits and the impact of marble waste on environmental pollution," J. Environ. Manage., vol. 87, pp. 106–116, 2008. https://doi.org/10.1016/J.JENVMAN.2007.01.004.

[14] A.G. Türkmenoğlu, A. Tankut, "Use of tuffs from central Turkey as admixture in pozzolanic cements: Assessment of their petrographical properties," Cem. Concr. Res., vol. 32, pp. 629–637, 2002. https://doi.org/10.1016/S0008-8846(01)00734-7.

[15] N.E. Altun, "Assessment of marble waste utilization as an alternative sorbent to limestone for SO2 control," Fuel Process. Technol., vol. 128, pp. 461–470, 2014. https://doi.org/10.1016/J.FUPROC.2014.08.009.

[16] H.Y. Aruntaş, M. Gürü, M. Dayi, I. Tekin, "Utilization of waste marble dust as an additive in cement production," Mater. Des., vol. 31, pp. 4039–4042, 2010. https://doi.org/10.1016/J.MATDES.2010.03.036.

[17] A. Hatice, "Investigation of fluidizing chemical additive compatibility of composite cements produced with yellow and grenn tuffs of Bayburt province," MS. Civil Eng., Bayburt Univ., 2020.

[18] ASTM C109, Standard Test Method for Compressive Strength of Hydraulic Cement Mortars, American Society for Testing and Materials, 2013.

[19] I. Tekin, T. Kotan, A.T. Osmanson, W. Brostow, O. Gencel, G. M. Barrera, “Properties of Lightweight Concrete Blocks with Waste Zeolitic Tuff”, Materials Science (Medžiagotyra). vol. 26, no. 4. 2020. https://doi.org/10.5755/j01.ms.26.4.22777